JOURNAL OF GEOPHYSICAL RESEARCH, VOL. 106, NO. E8, PAGES 17,579-17,587, AUGUST 25, 2001

Magnetic Properties Experiments on the Mars Polar Lander

C. T. Mogensen,[1] J. M. Knudsen,[1] M. B. Madsen,[1] P. Bertelsen,[1] S. F. Hviid,[1]
R. B. Hargraves,[2] P. Smith,[3] and D. A. Paige[4]

Abstract. The Mars Polar Lander carries an instrument package called the Magnetic Properties Experiments. This package consists of one magnet array, one tip-plate magnet, and three Thermal and Evolved Gas Analyzer (TEGA) magnets. The magnet array and the tip-plate magnet are identical to those flown on Mars Pathfinder and will be passively exposed to airborne dust. The TEGA magnets are a new addition to the package designed to study actively sampled material collected from three different depths in the trench that will be dug by the robotic arm soil sampler.

1. Introduction

The landing site of Mars Polar Lander (MPL) will be at a latitude of about 77° south, far from the landing sites of the Viking landers (23° and 48° north) and Mars Pathfinder (20° north). To determine whether this difference affects in any way the magnetic properties of the airborne dust and because MPL will sample the soil directly, it was decided to send magnets on the mission. The Magnetic Properties Experiments (MPE) package on MPL will include three types of instruments. Two of these are identical to those on Mars Pathfinder, with a third type to take advantage of the active soil sampling.

The two instruments inherited from Pathfinder are a magnet array and a tip-plate magnet. These instruments consist of permanent magnets, which will be passively exposed to the airborne dust, and will attract magnetic particles suspended in the atmosphere. The magnets will be periodically viewed by the Surface Stereo Imager (SSI) and the pictures will be transmitted to Earth. These pictures are the data on which conclusions on the magnetic properties of the airborne dust will be based.

The magnet array, placed about 1 m from the SSI, consists of five small "bull's-eye" permanent magnets embedded in magnesium metal. The magnets are of very different strengths. The weakest magnet is about 1000 times weaker than the strongest magnet. The tip-plate magnet consists of a single strong permanent magnet placed about 7 cm from the right eye of the SSI. The constructions of the magnet array and the tip-plate magnet are described in detail elsewhere, in connection with the Mars Pathfinder Mission [*Smith et al.*, 1997; *Gunnlaugsson et al.*, 1998].

[1]Ørsted Laboratory, Niels Bohr Institute for Astronomy, Physics and Geophysics, University of Copenhagen, Denmark.
[2]Department of Geosciences, Princeton University, Princeton, New Jersey.
[3]Lunar and Planetary Laboratory, University of Arizona, Tucson.
[4]Department of Earth & Space Sciences, University of California, Los Angeles.

Paper number 1999JE001077.
0048-0227/01/1999JE001077$9.00

The third type of instrument in the MPE package is a magnet specifically designed to examine material sampled by the robotic arm (RA). The TEGA magnets (as they are called) will be described in detail below. These magnets are named after the instrument onto which they are attached, the Thermal and Evolved Gas Analyzer (*W. V. Boynton et al.*, Thermal and Evolved Gas Analyzer: Part of the Mars Volatile and Climate Surveyor integrated payload, submitted to Journal of Geophysical Research, 1999). There will be three TEGA magnets, one on each of the cells of the TEGA that are facing the SSI. Thus imaging of the TEGA magnets will be possible using both the SSI and the robotic arm camera (RAC). With a resolution of the RAC better than 100 μm at the distance anticipated when the scoop of the RA is kept free of the TEGA instrument, this camera will be able to supply excellent close-up images of patterns of material captured by the TEGA magnets.

From the Viking and Pathfinder missions it has been established with certainty that the airborne dust on Mars contains a ferrimagnetic mineral [*Hargraves et al.*, 1977, 1979; *Hviid et al.*, 1997; *Madsen et al.*, 1999]. Both Viking landers carried a scoop designed to collect samples of the Martian surface material for analyses by instruments in the lander. Two permanent magnets were attached to the backhoe beneath the scoop, and these magnets were inserted directly into the surface material each time a sample was collected. From the results of the Magnetic Properties Experiments on the Viking landers it was established that not only the dust in the atmosphere but also the surface material of the planet must contain a strongly magnetic (ferrimagnetic) phase [*Hargraves et al.*, 1977, 1979]. Together with the results from the Pathfinder mission, the main conclusion concerning the magnetic properties of the surface material of Mars is that the dust suspended in the Martian atmosphere, as well as the surface soil of Mars, contains a ferrimagnetic mineral present as an accessory component in most, if not all, of the particles. From Pathfinder data it is estimated that the reddish Martian surface material has an average magnetization of about 4 A m^2 kg^{-1} [*Hviid et al.*, 1997; *Madsen et al.*, 1999].

The Viking backhoe magnets were inserted into the top layer of the Martian surface soil. Whether the magnetic properties are characteristic of this surface soil alone or whether the material at greater depths is also magnetic is not

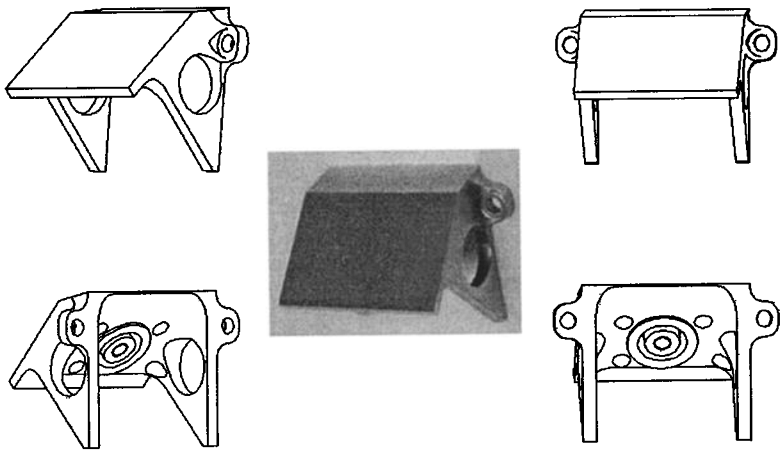

Figure 1. A Thermal and Evolved Gas Analyzer magnet. The instrument consists of a 4 mm thick rectangular aluminum plate with a series of permanent magnets embedded in it. The magnets are not visible from the outside. When mounted on the TEGA analyzer, the plate is tilted 45° from horizontal. The "wings" and "ears" are used for mounting.

known. The robotic arm on Mars Polar Lander will sample material from depths of up to perhaps half a meter.

The TEGA magnet is designed to be used for studies of the magnetic properties of soils sampled by the robotic arm on Mars Polar Lander. Putative magnetic particles of the subsurface soil may be very weakly magnetic. For example, the magnetic mineral may be completely embedded in particles consisting mainly of water ice. Such composite particles will have a low bulk saturation magnetization. The TEGA magnet is therefore designed with the capability to attract particles with a low average magnetization.

2. Position of the TEGA Magnet

As described in detail below, the TEGA magnet consists of several permanent magnets embedded in an aluminum structure. Figure 1 shows a picture of the magnet before it is mounted on the TEGA housing. The active area of the magnet is an aluminum plane of dimensions 23 by 18 mm. The other part of the aluminum structure is used for mounting the magnet.

Consider Figure 2. The soil that is delivered by the robotic arm to the TEGA is dumped onto a sieve of aperture size 0.9 mm. The sieve is inclined 45° relative to the horizontal plane. It is assumed that sample delivery will be centered on the sieve, i.e., that the majority of the sample will fall in the central third of the area of the sieve. Particles too large to pass through the sieve move down the incline and off the TEGA housing. The motion of the particles down the inclined plane is complicated. The particles will roll, slide, and jump on their way down, and the large particles will cause also smaller particles to reach the end of the incline. How far below the runoff point of the inclined plane should the magnet be placed?

It is desirable that as much as possible of the sample delivered to the TEGA instrument and not penetrating the sieve will encounter the magnet in falling. We have therefore based the decision of the positioning of the TEGA magnet on the following conservative criterion. Consider a particle that is placed two thirds of the way up the inclined plane and which thereafter slides without friction down the plane. When the particle leaves the inclined plane, it will fall freely in the gravitational field of Mars. The TEGA magnet is located in a position such that this particle will just hit the far edge of the magnet. It is assumed that the majority of the sample will be delivered below the point considered above (and that friction

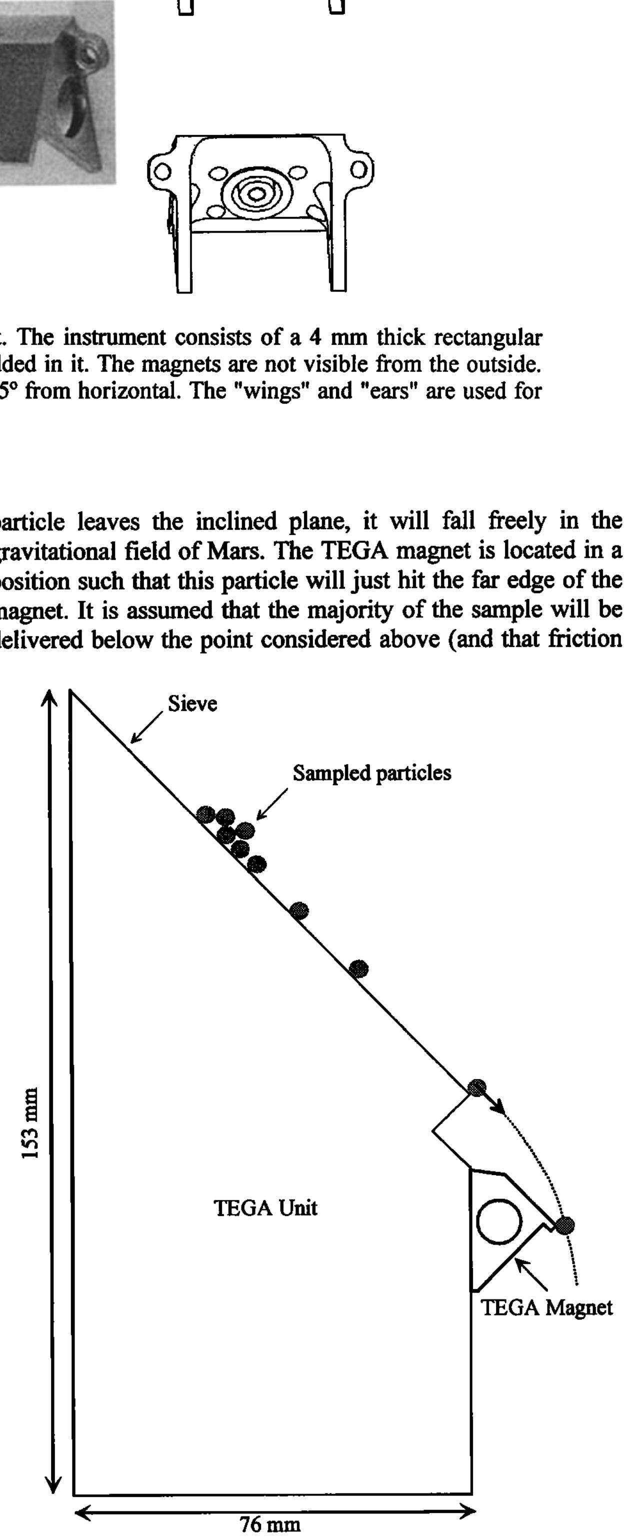

Figure 2. A soil sample being delivered to an analyzer cell of the TEGA. The TEGA magnet is placed below the inclined plane, which consists of a sieve. Some particles pass through the holes in the sieve, and some particles reach the magnet. If sufficiently magnetic, the particles may be captured by the magnet.

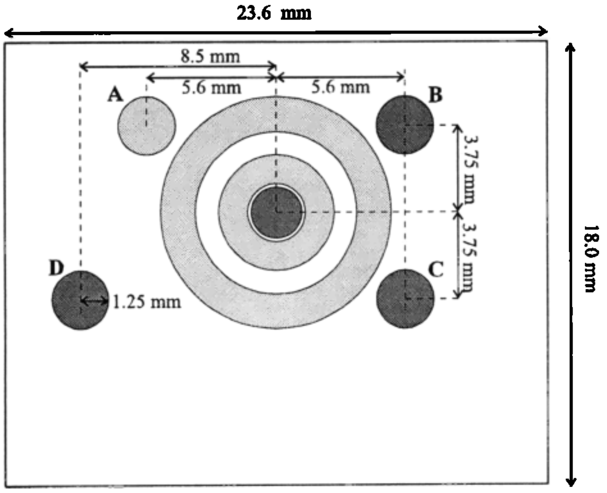

Figure 3. The internal structure of a TEGA magnet, showing the geometry and positions of the magnetic material that is embedded in the aluminum structure of the instrument. The instrument contains a central strong magnet assembled from two concentric rings and a rod, all 4.0 mm thick. The four satellite magnets consist of 0.4 mm thick discs. Darker colored units are magnetized with their north poles out of the paper; lighter colored units are oppositely magnetized.

and interaction among particles will play a role). This criterion will ensure that a majority of the sampled particles will be exposed to the active surface of the TEGA magnet.

It should be noted that the path of the hypothetical particle considered above, extrapolated to the lander instrument deck and the bottom of the TEGA instrument, coincides exactly with the outer limits of the "dirt area" surrounding the TEGA instrument. The "dirt area" is the area of the lander deck that has been kept free for the purpose of being used as a deposition area for the spillover from the samples delivered to the TEGA.

3. Design of the TEGA Magnet

The active part of the TEGA magnet consists of several small samarium-cobalt (Sm_2Co_{17}) magnets embedded in the aluminum structure. The saturation magnetization of Sm_2Co_{17} is 8.75×10^5 A m^{-1}. The positioning of the magnetic material below the active surface is illustrated in Figure 3. Figure 3 shows both the geometry and the position of the different units of magnetic material. The main structure is a central strong magnet assembled from two concentric rings and a rod, all 4.0 mm thick. Darker colored units are magnetized with their north poles out of the plane of the paper; lighter colored units are oppositely magnetized. The samarium-cobalt permanent magnets are placed either 0.4 or 0.7 mm below the active surface of the instrument (see Table 1). The particles will roll over the active surface of the magnet and get attracted, if they contain sufficient magnetic material.

Positioned outside this configuration are four satellite magnets, denoted A, B, C, and D. The positioning, the dimensions, and the direction of magnetization of these satellite magnets are all apparent from Figure 3. In Table 1 the magnetization directions of the different components relative to the inner rod are given. The dimensions and positions of the magnets are also given in Table 1. We should perhaps remark that the characteristics of the TEGA magnet assembly would not be changed if the direction of magnetization of all components were reversed.

3.1. Characteristics of the TEGA Magnet

Considering the fact that the particles will tumble down the inclined plane and pass over the active surface of the TEGA magnet, it is evident that the magnet should be strong, in order to attract also weakly magnetic particles. The word strong here includes two aspects: the ability to attract and the ability to hold magnetic particles. As described below, these two properties of a magnet somewhat counteract each other.

For single-domain magnetic particles, or particles that are saturated magnetically, the force F_z on a particle oriented in the z direction of a given coordinate system, is given by $F_z = m\ \sigma_S\ (dB_z/dz)$; that is, the force is proportional to the mass m, the specific saturation magnetization σ_S, and the magnetic field gradient.

For nonsaturated magnetic particles, oriented in the z direction of a coordinate system, the force is given by $F_z = m\ \kappa_i/\mu_0\ B_z\ (dB_z/dz)$; that is, the force is proportional to the product of the magnetic field and the magnetic field gradient ($\mu_0 = 4\pi \times 10^{-7}$ V s A^{-1} m^{-1} and κ_i is the specific magnetic susceptibility (unit: m^3 kg^{-1})).

When optimizing the ability of a magnet to hold a magnetic particle already sitting on the surface, the magnet must have a large field gradient. When the magnetic field gradient in the vicinity of the surface of the magnet is large, the magnetic field is decreasing rapidly when moving away from the surface of the magnet. The ability of the magnet to attract a particle "far" from the magnet is strongly dependent on the magnetic field, which orients the particles along the field lines and magnetizes nonsaturated particles. Said in another way, the capture cross section of the magnet is large if the magnetic field is large [*Madsen et al.*, 1999].

The TEGA magnet is designed to have both a substantial magnetic field and a large magnetic field gradient. This has been accomplished in the following way. The inner cylindrical magnet, i.e., the rod, and the inner ring have been

Table 1. Dimensions of Different Components of the TEGA Magnet

Magnet Component	r, mm	b, mm	z, mm	Magnetization
Rod	1.10	4.0	0.41	normal to surface
Inner ring	1.25 - 2.50	4.0	0.41	antiparallel direction
Outer ring	3.50 - 5.00	4.0	0.41	antiparallel direction
Satellite A	1.25	0.5	0.71	antiparallel direction
Satellite B	1.25	0.5	0.41	parallel direction
Satellite C	1.25	0.5	0.41	parallel direction
Satellite D	1.25	0.5	0.71	parallel direction

assembled with as little distance between the two magnets as possible. See Figure 3. The two magnets are magnetized in opposite directions, which gives rise to a large magnetic field gradient in the inner parts of the TEGA magnet. The central region of the magnet will thus be able to hold particles that, for instance, consist of ice and a small amount of ferrimagnetic material. Outside the central region a second concentric ring magnet is placed. The outer ring is magnetized in the same direction as the inner ring. This makes sure that the magnetic field decreases comparatively slowly when moving away from the surface of the magnet. With this somewhat complicated construction the TEGA magnet has a good ability to capture magnetic particles (a large capture cross section) and at the same time a good ability to hold particles that have already reached the surface of the magnet (a large field gradient). With the mass allocated (each TEGA magnet weighs 6.93 g), it would have been possible to make the magnetic field gradient or the capture cross section larger, but either would have compromised the overall strength of the magnet.

3.2. Satellite Magnets

The nature of the material sampled by the robotic arm and placed on the TEGA housing is, of course, not known. Will the material be dust-sized particles (< 20 μm), or will it be very coarse grained? If the material is fine grained, more knowledge of its magnetic properties may be obtained if small satellite magnets are added to the central ring magnet system.

The four satellite magnets have the effect of modifying the magnetic field and magnetic field gradient around the central disc and ring system, thereby modifying the pattern of attracted dust on the surface of the magnet. The way the different satellite magnets modify the dust pattern is described below. Consult again the drawing of the internal structure of the TEGA magnet. To ease the discussion in the following, the rod, the inner ring, and the outer ring are named 1, 2, and 3, respectively (see Figure 4). Also shown are three lines going from the center of the rod and ring system through the centers of three of the satellite magnets (magnets A, B, and D).

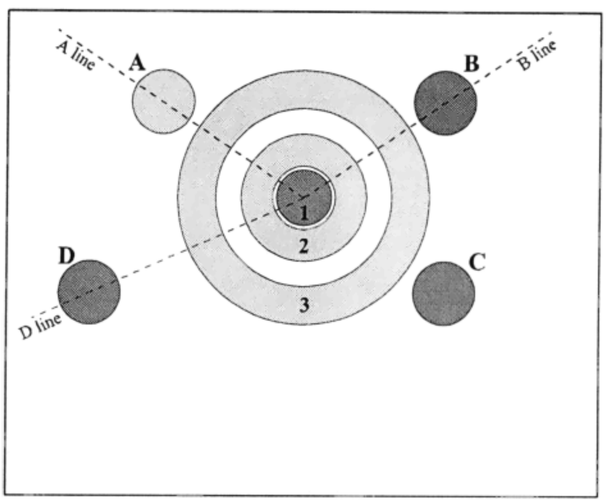

Figure 4. To illustrate the properties of the satellite magnets (A, B, C, and D), the radial and vertical components of the magnetic field and magnetic field gradient will be shown in Figures 5 and 6. The fields will be displayed as their magnitudes on the surface of a TEGA magnet along the lines A, B, and D.

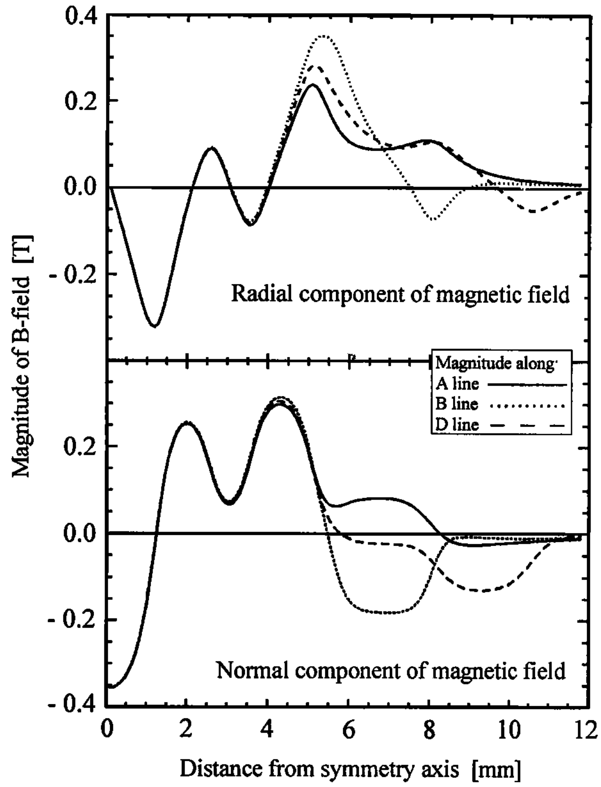

Figure 5. The radial and vertical components of the magnetic field along the lines A, B, and D defined in Figure 4.

The characteristics of the four satellite magnets are the following. Magnet A is positioned just outside of ring 3 and with the same magnetization as this ring. Magnet B is situated at the same distance but with opposite magnetization. Magnet C has the same distance and magnetization as magnet B but with the difference that it is positioned below a horizontal line passing through the center of the disc and ring system. Magnet D is positioned a distance of 1.4 times the distance of the other satellite magnets and with the same magnetization as magnets B and C. Some of the effects of this configuration on the magnetic field and magnetic field gradient can be seen in Figure 5. In Figure 5 the radial (top) and normal (bottom) components of the magnetic field at the outer surface of the aluminum structure, i.e., at the active surface of the TEGA magnet, are plotted as a function of the distance from the center (symmetry axis) of the disc and ring system. The peak value of the field is about 350 mT. The corresponding field of the strongest magnet on the Pathfinder magnet array is 280 mT.

The magnetic fields shown in Figures 5 and 6 are results of numerical calculations based on the known properties of the magnetic material used for the magnets. These calculations have been verified by measurements with a Hall probe at different distances above the surface of the TEGA magnet.

In Figure 6 the magnetic field gradient on the surface of the magnet has been plotted as a function of the distance from the symmetry axis. The radial component of the magnetic field

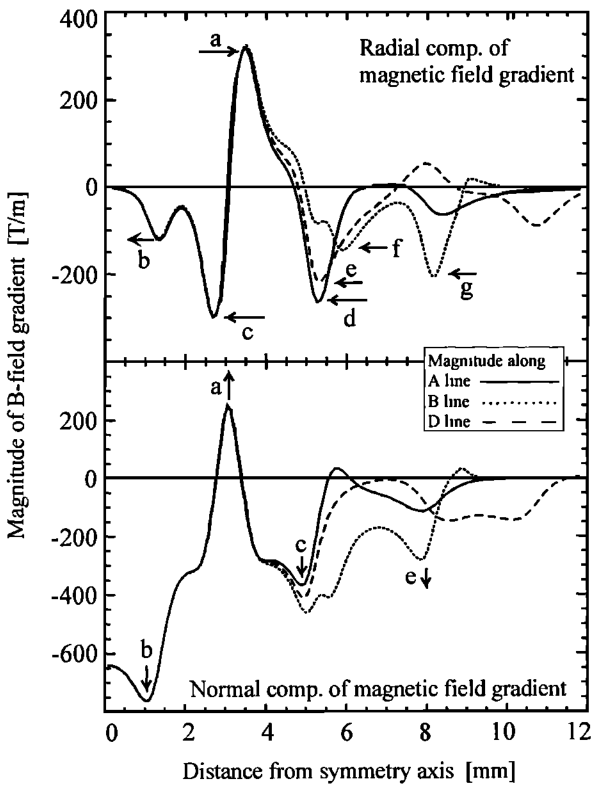

Figure 6. The radial and vertical components of the gradient of the magnetic field along the lines A, B, and D defined in Figure 4.

gradient (Figure 6, top) is proportional to the force, parallel to the active surface of the instrument, on a magnetic particle. When the curve is negative, it means that the force is directed toward the center of the rod and ring system. For positive values the force is directed radially away from the center. The arrow marked a in Figure 6 (top) indicates a region where magnetic particles are pushed outward toward the inner radius of ring 3. The arrow marked c shows that magnetic particles are pulled inward toward the outer radius of ring 2. If the particles attracted are small enough, this will clear the area between rings 2 and 3 effectively, and a distinct "bulls-eye" pattern will be visible. A similar effect, although not as evident, can be seen in the small gap between rod 1 and ring 2 (indicated by the arrow marked b).

The difference between magnets A and B becomes clear when looking at the arrows d, f, and g. Magnet A has the effect that the magnetic particles accumulate at the outer radius of ring 3 (in the gap between magnet A and ring 3), while magnet B makes the particles accumulate on the edge of magnet B itself, both at the inner edge (arrow f) and even more evident at the outer edge (arrow g). It should be noted that all attractive forces from magnets A and B pull magnetic particles toward the center of the rod and ring system. The effect of magnet D can be seen in the dashed line in Figure 6 (top). Arrow e shows that the particles are attracted to the outer radius of ring 3. Furthermore, it can be seen that magnet D has the effect of pushing particles away from ring 3, thereby cleaning the region between ring 3 and magnet D.

Figure 6 (bottom) shows the vertical component of the magnetic field gradient, on the surface of the TEGA magnet. As seen from the figure, the peak value of the vertical magnetic field gradient is about 750 T m^{-1}. This is a very large magnetic field gradient. The similar field gradient on the strongest magnet on the Pathfinder magnet array was about 130 T m^{-1}. Arrow b shows the regions where the attractive force is particularly large, i.e., in the gap between disc 1 and ring 2 and at the inner radius of ring 3. This corresponds well with the region the magnetic particles are pushed toward by the effect of the radial component of the magnetic field gradient, according to Figure 6 (top). The most noticeable difference between magnets A and B, in Figure 6 (bottom), is that magnet B has a much larger attractive force on the position of the satellite magnet, the outer and inner radius shown as arrows c and e.

The purpose of magnet C is to see if there is any difference between the pattern of dust on magnet B and that of magnet C due to the effect of the gravitational pull on Mars. The only difference in the configuration of these magnets is that one (magnet B) is placed above a horizontal line going through the center of the rod and ring system and the other (magnet C) is placed symmetrically below this line. If the effect of friction between a magnetic particle and the surface of the magnet is much larger that the effect due to the gravitational force, the patterns on the two magnets will appear similar. If, however, the friction force is small, compared to the gravitational force on the particle, this will show up as a significant difference between these patterns. As a particle landing near magnet B will be attracted toward the disc and ring system, a component of the gravitational force on the particle will act in the same direction as the magnetic force. If, on the other hand, a particle lands near magnet C, a component of the gravitational force and the magnetic force acting on the particle will act in two opposing directions. More particles will therefore be able to find a stable position just above magnet C where the particles are pulled up by the magnetic force from ring 3 and pulled down by the gravitational force. That is not the case for magnet B. A particle sitting just above magnet B will be pulled down by the magnetic force from ring 3 and by the gravitational force both working in the same general direction.

3.3. Attraction of Airborne Magnetic Particles by the TEGA Magnet

We have performed a series of simulation experiments using magnetic particles of different linear dimensions and of different specific magnetization. For illustration, we first consider a few examples of magnetic particles with dimensions substantially lower ($d \sim 10$ μm) than the dimensions of the TEGA magnet. A large fraction of particles with such dimensions will, when brought to the TEGA magnet, fall through the sieve. As shown in section 3.4., small particles delivered to the TEGA housing may, however, be attracted by the TEGA magnet, due to the fact that the small particles may be dragged down the inclined plane via larger particles.

As a contingency, the TEGA magnets could be used to study airborne material as well. The TEGA magnet will, when the TEGA cover is opened, attract airborne dust. It should be stressed that the TEGA magnet is not designed to attract magnetic particles from the dust suspended in the Martian atmosphere.

In this section we briefly consider the effect of the TEGA magnet on small magnetic particles that are blown onto the

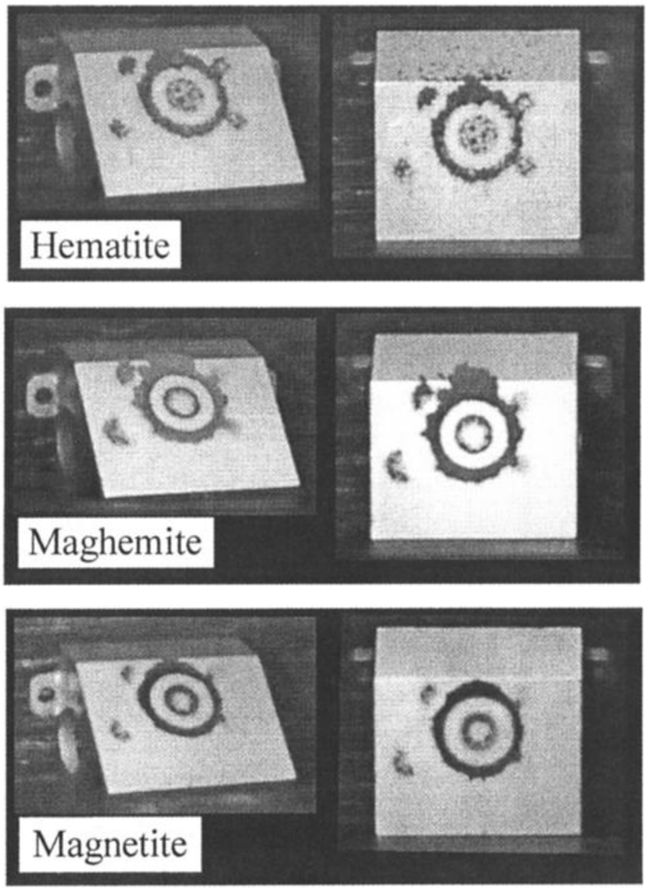

Figure 7. Patterns formed on the TEGA magnet by particles of the minerals hematite, maghemite, and magnetite blown onto the TEGA magnet in the laboratory. In the images at the right the magnet is imaged as it would be, seen from the robotic arm camera (RAC).

magnet in the laboratory. For this purpose the TEGA magnet was placed in a transparent plastic container of dimensions 40 by 30 by 10 cm. A fan is placed inside the container. The dust to be studied is placed into the container in the desired amount, and then the fan is activated. The dust is thus stirred up, and, if sufficiently magnetic, it is attracted to the magnet.

The TEGA opening (and the magnet) is protected from contamination by a cover until just before a sample is going to be delivered to the TEGA chamber. The laboratory simulation experiments where dust is blown onto the magnet are for illustration purposes only. However, see section 3.4.

Figure 7 shows a few examples illustrating the results of the laboratory simulation experiments. The top figure is the result of hematite (α-Fe_2O_3, $d \sim 10$ μm) blown onto the TEGA magnet. Hematite has a saturation magnetization of $\sigma_S = 0.4$ A m^2 kg^{-1}. The center figure is the analogous experiment for maghemite (γ-Fe_2O_3, $d \sim 10$ μm, $\sigma_S = 70$ A m^2 kg^{-1}) and the bottom figure is magnetite (Fe_3O_4, $d < 10$ μm, $\sigma_S = 92$ A m^2 kg^{-1}).

The TEGA magnet is strong; therefore, despite the large difference in saturation magnetization, the results of the experiments for hematite, maghemite, and magnetite show similarities. There are though differences in the pictures shown in Figure 7. With maghemite and magnetite the central part of the inner magnet is cleaned. This is mainly due to the fact that these minerals have a much higher saturation magnetization than hematite. There are also subtle differences in the covering of the satellite magnets. In the case of maghemite/magnetite, nearly all the dust of the two satellite magnets B and C is pulled into the ring magnet, because of the high saturation magnetization. Also, differences in the coefficient of friction for the particles of hematite, maghemite, and magnetite play a role.

From such images it is possible to distinguish between minerals with large saturation magnetization and minerals with small saturation magnetization. Distinguishing between, for example, maghemite and magnetite is not possible without using the robotic arm camera (RAC) color lamps to obtain color images of the material on the TEGA magnets.

3.4. Simulation Experiments: Particles Sliding Down the Sieve of the TEGA

The chemical and physical properties (including magnetization) of the material sampled from various depths of the Martian surface and brought to the TEGA for analysis are not known. The material may contain ferrimagnetic particles

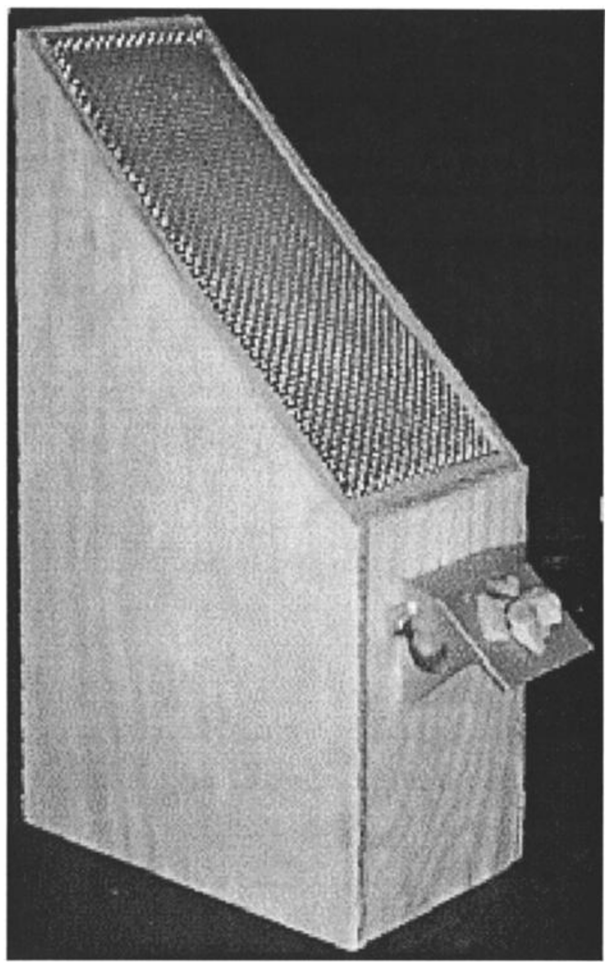

Figure 8. A TEGA analyzer cell mock-up used for simulation of the Magnetic Properties Experiment. The blocks appearing on the surface of the TEGA magnet are 6% maghemite embedded in plaster of Paris and are caught by the TEGA magnet when rolling from the sieve of the analyzer cell.

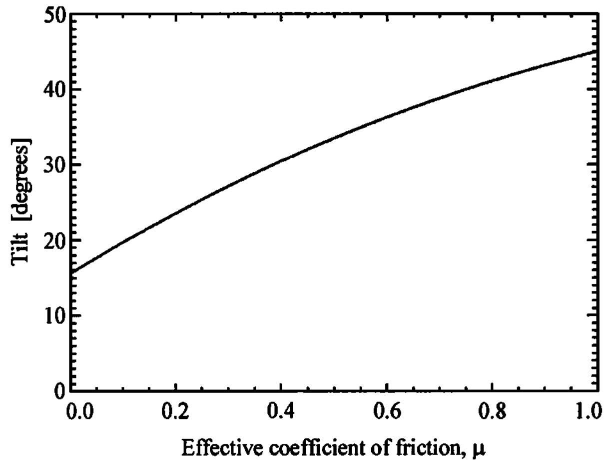

Figure 9. The tilt angle θ_E of the surface of the sieve of the analyzer cell as a function of the effective coefficient of friction μ between the sieve and moving particles to simulate in the laboratory the influence of the lower gravity on Mars.

(maghemite, titanomagnetite) intergrown with nonmagnetic particles or even ferrimagnetic particles embedded in water ice or CO_2 ice.

To simulate the active magnetic properties experiment, we have produced a series of intergrown particles with variable contents of ferrimagnetic minerals and variable particle size distributions. The particles are made by carefully mixing plaster of Paris ($CaSO_4 \cdot 1/2\ H_2O$) with the desired amount of a ferrimagnetic mineral, for example, maghemite. By adding a small amount of water to the mixture, a suspended compound is created, which will harden after some hours. When the material has hardened, it is crushed to the desired mixture of particle sizes in a mortar. We then have a sample ready for the simulation experiment. Figure 8 shows a wooden box with the same shape and dimensions as the TEGA housing. The sieve covering the housing is produced from the same material that is used in the flight unit of the TEGA. The position of the TEGA magnet is clearly seen. The magnet has captured a few large particles that have slid down the inclined plane after having been placed at the top of the sieve. The particles

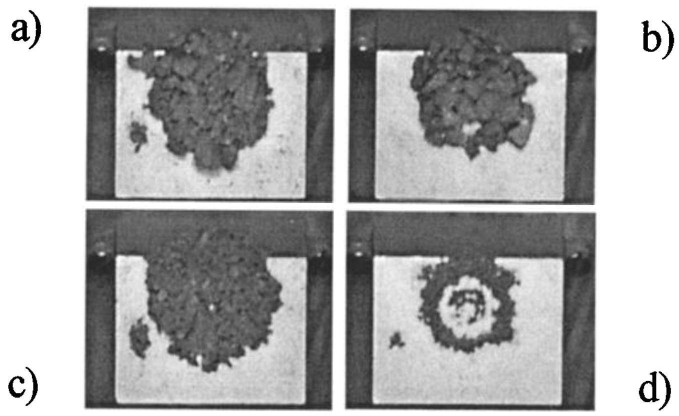

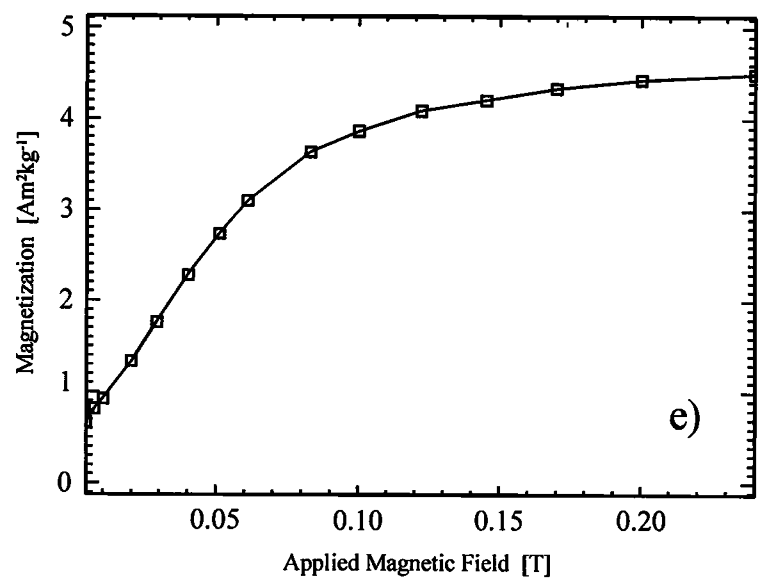

Figure 10. Patterns formed on the TEGA magnet by sampling falling particles of 6% maghemite embedded in plaster of Paris: (a) particles as produced, (b) particles larger than sieve aperture, (c) particles smaller than sieve aperture, and (d) particles as in Figure 10c but delivered very slowly to the sieve. (e) The magnetization curve for 6% maghemite embedded in plaster of Paris.

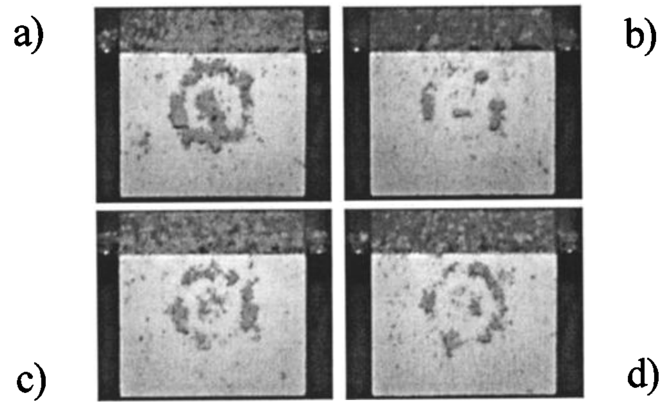

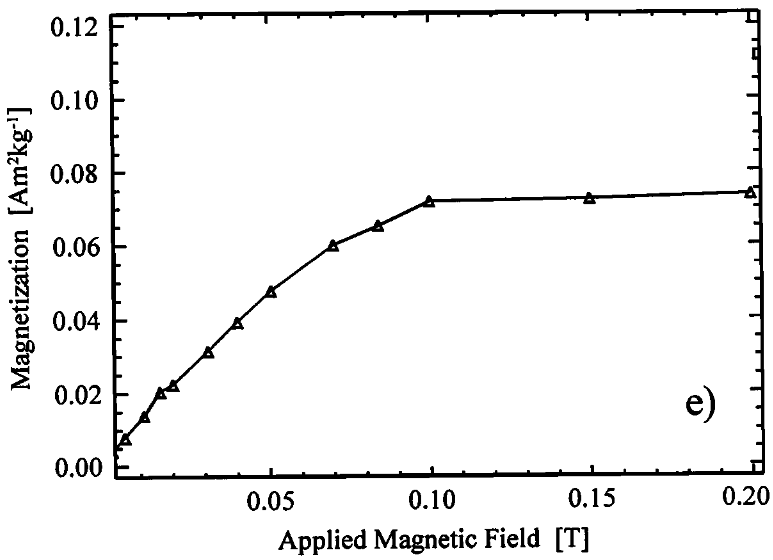

Figure 11. Patterns formed on the TEGA magnet by sampling falling particles of 0.1% maghemite embedded in plaster of Paris: (a) particles as produced, (b) particles larger than sieve aperture, (c) particles smaller than sieve aperture, and (d) particles as in Figure 11c but delivered very slowly to the sieve. (e) The magnetization curve for 0.1% maghemite embedded in plaster of Paris.

contain 6% by weight of maghemite, resulting in a saturation magnetization for the particles of $\sigma_S = 4$ A m^2 kg^{-1}.

In simulation experiments with the TEGA magnet on Earth, a set of parameters are different from the parameters for corresponding experiments on Mars. The acceleration due to gravity on Mars is $g_M = 0.38\ g_E$, where g_E is the acceleration due to gravity on Earth ($g_E = 9.8$ m s^{-2}). When performing simulation experiments on Earth, we have decided to incorporate a different geometry in the setup to compensate for the larger gravitational pull on Earth. We simply change the angle of inclination, θ_E, to the horizontal. The change necessary is estimated in the following way. Consider a particle of mass m sliding down the sieve of the TEGA housing. Let the coefficient of friction between the particle and the sieve be μ. For a realistic laboratory simulation experiment we have the following equation, which governs the connection between the inclination angle on Earth, θ_E, and the inclination angle on Mars, θ_M:

$$m\, g_E \sin\theta_E - \mu\, m\, g_E \cos\theta_E = m\, g_M \sin\theta_M - \mu\, m\, g_M \cos\theta_M.$$

As $\theta_M = 45°$, we can, for a given value of μ, determine the corresponding inclination angle θ_E on Earth. Figure 9 shows, for the TEGA sieve surface on Earth, the tilt angle θ_E required to simulate the experiment in Mars gravity as a function of the friction coefficient μ. Given the complicated motion of the particles down the inclined plane, and given the fact that the coefficient of friction is a function, not only of the material used but also of the particle shape, the results concerning the tilt are at best semiquantitative. In the laboratory simulation experiments we have used a tilting angle of 36°, corresponding to a coefficient of friction $\mu \sim 0.6$.

Figure 10 shows the results of particles of different size poured onto the sieve in the same manner as it will be done on Mars. The particles contain 6% of maghemite by weight giving a saturation magnetization of $\sigma_S = 4$ A m^2 kg^{-1}. This corresponds to the estimated saturation magnetization of the surface soil of Mars [*Hargraves et al.*, 1979; *Hviid et al.*, 1997; *Madsen et al.*, 1999].

Figure 10a shows the particles as produced, and Figure 10b shows particles that are too large to fall through the sieve. If, however, a sufficient amount of small particles is poured onto the sieve, some of the particles will reach (and be attracted to) the magnet. In Figure 10c a large amount of material has been dumped onto the sieve, and the magnet is completely covered by captured material. If a smaller amount of material is continuously placed on top of the sieve, less material will be attracted to the magnet, as shown in Figure 10d. Note that in all three cases where the material contains small particles, some of these have been attracted to the satellite magnet designated D in Figure 3. Figure 10 includes a curve showing the magnetization of the material poured onto the sieve. The magnetization is measured in a vibrating sample magnetometer and gives the specific magnetization as a function of an impressed magnetic field *B*. The saturation magnetization, which is about 4 A m^2 kg^{-1}, is reached for an impressed magnetic field of $B = 0.1$ T.

Figure 11 shows results from corresponding experiments with composite particles containing 0.1% of maghemite by weight. After crushing, this gives particles with a specific saturation magnetization of σ_S = 0.07 A m^2 kg^{-1}. See the magnetization curve of Figure 11. The material is magnetically saturated in a field of about 0.1 T. The magnetic susceptibility is approximately κ_i = 10^{-6} m^3 kg^{-1}, magnetization curve of Figure 11. The material is magnetically saturated in a field of about 0.1 T. The magnetic susceptibility is approximately κ_i = 10^{-6} m^3 kg^{-1}, corresponding to the initial susceptibility of many terrestrial basalts. In spite of the fact that a large amount of material was poured onto the sieve, only a small part was captured by the magnet. The particles captured may also have a somewhat higher magnetization because of the fact that it is difficult to make the suspension of maghemite in plaster of Paris completely homogeneous in this low concentration. In the batch used we have found particles with saturation magnetization of σ_S = 0.1 A m^2 kg^{-1}. Our simulation experiments show that an amount of about 0.1% of a ferrimagnetic mineral contained in the surface material corresponds to the lower limit of detection.

We have prepared a catalogue of pictures for various values of saturation magnetization and particle size distributions. The catalogue will be used to aid interpretation of the pictures from the results of the experiments on Mars.

4. Conclusions

It is evident that from a crude magnetic properties experiment like the one described in this article it will be difficult to get a quantitative value of the average saturation magnetization of the material attracted to the TEGA magnet or a unique identification of the ferrimagnetic phase responsible. We will, however, have the opportunity to study material on Mars sampled from three different depths. As the TEGA magnet is designed, it will be possible to obtain a rough estimate of the average magnetization. The detection limit of the TEGA magnet is given by the fact that the magnet will be able to attract and hold particles containing a strongly ferrimagnetic phase in an amount larger than 0.1% by weight.

Acknowledgments. Our participation in the project is supported by the Danish Research Agency and by the (Danish) Foundation of 23. September 1909. C. T. Mogensen is supported by the Danish Space Research Institute. R. B. Hargraves is supported by NASA grant 960869.

References

Boynton, W.V., et al., The Thermal and Evolved Gas Analyzer: Part of the Mars Volatile and Climate Surveyor integrated payload, *J. Geophys. Res.*, this issue.

Coey, J.M.D., S. Mørup, M.B. Madsen, and J.M. Knudsen, Titanomaghemite in magnetic soils on Earth and Mars, *J.Geophys. Res.*, *95*, 14,423-14,425, 1990.

Gunnlaugsson, H.P., S.F. Hviid, J.M. Knudsen, and M.B. Madsen, Instruments for the Magnetic Properties Experiments on Mars Pathfinder, *Planet. Space Sci.*, *46*,449-459, 1998.

Hargraves, R.B., D.W. Collinson, R.E. Arvidson, and C.R.Spitzer, The Viking Magnetic Properties Experiment: Primary mission results, *J. Geophys. Res.*, *82*, 4547-4558, 1977.

Hargraves, R.B., D.W. Collinson, R.E. Arvidson, and P.M. Cates, Viking Magnetic Properties Experiment: Extended mission results, *J. Geophys. Res.*, *84*, 8379-8384, 1979.

Hviid, S.F., et al., Magnetic Properties Experiments on the Mars Pathfinder Lander· Preliminary results, *Science*, *278*, 1768-1770, 1997.

Madsen, M.B., S.F. Hviid, H.P. Gunnlaugsson, W. Goetz, C.T. Pedersen, A.R. Dinesen, C.T. Mogensen, M. Olsen, and R.B. Hargraves, The Magnetic Properties Experiments on Mars Pathfinder, *J. Geophys. Res.*, *104*, 8761-8779, 1999

Smith, P.H., et al., Results from the Mars Pathfinder Camera, *Science*, *278*, 1758-1765, 1997.

P. Bertelsen, S. F. Hviid, J. M. Knudsen, M. B. Madsen and C. T. Mogensen, Ørsted Laboratory, Niels Bohr Institute for Astronomy, Physics and Geophysics, University of Copenhagen, Universitetsparken 5, DK-2100 Copenhagen Ø, Denmark. (preben@fys.ku.dk; stubbe@fys.ku.dk; knudsen@fys.ku.dk; mbmadsen@fys.ku.dk; tilsted@fys.ku.dk)

R. B. Hargraves, Department of Geosciences, Princeton University, Princeton, NJ 08450.

D. A. Paige, Department of Earth and Space Sciences, University of California, Los Angeles, CA 90032.

P. Smith, Lunar and Planetary Laboratory, University of Arizona, Tucson, AZ 85721.

(Received April 28, 1999; revised October 12, 1999; accepted October 19, 1999)